



Real-world emissions of nanoparticles, particulate mass and black carbon from a plug-in hybrid vehicle compared to conventional gasoline vehicles

P. Karjalainen^{a,*}, V. Leinonen^b, M. Olin^a, K. Vesisenaho^a, P. Marjanen^a, A. Järvinen^{a,1},
P. Simonen^a, L. Markkula^a, H. Kuuluvainen^a, J. Keskinen^a, S. Mikkonen^{b,c}

^a Aerosol Physics Laboratory, Tampere University, P.O. Box 692, 33014 Tampere, Finland

^b Department of Technical Physics, University of Eastern Finland, P.O. Box 1627, 70211 Kuopio, Finland

^c Department of Environmental and Biological Sciences, University of Eastern Finland, P.O. Box 1627, 70211 Kuopio, Finland

ARTICLE INFO

Keywords:

Plug-in hybrid electric vehicle
Gasoline vehicle
Particle emission
particle number
Particle mass
Black carbon

ABSTRACT

Among various Hybrid Electric Vehicles (HEVs), Plug-in Hybrid Electric Vehicles (PHEVs) charged from the grid are seen as the most advanced ones, as they can drive dozens of kilometers using only the electric engine and thus producing less tailpipe greenhouse gas emissions than vehicles with internal combustion engines or other HEVs. The proportion of PHEVs among all vehicles is still relatively low but increasing rapidly in many countries. However, the real-world emissions from these novel hybrid technologies are not straightforward to estimate. This study investigates multiple properties of the particle emissions of a PHEV, with gasoline direct injection, GDI, compared to two conventional gasoline vehicles, one with port fuel injection, PFI and one with GDI. Distance-based emission factors (EFs) for each vehicle in various driving modes, including battery-hold and battery-charge driving modes for the PHEV, were analyzed. The results showed that the PHEV produced smaller particles in size, resulting that particle mass (PM) and black carbon (BC) were lower by factor of ten in comparison to EFs from the vehicles with PFI and GDI engines. The PHEV consistently emitted lower distance-based EFs than the PFI and GDI vehicles in all driving modes, though EF for particle number (PN) in battery-charge mode was close to the EFs from the other two vehicles. The study also found that the vehicle cold start effect was present in the case of the shorter driving route but not as significant in the longer one. Overall, the study demonstrated that PHEVs could produce lower particle and BC emissions compared to traditional gasoline-powered vehicles. The vehicle cold start and systematic combustion engine restart effects still can have significant impacts on particle emissions, especially in shorter trips.

Introduction

Road traffic electrification is currently seen as the main action for decreasing the GHG (greenhouse gas) emissions from traffic and improving the air quality in cities and roadsides. As rapid transformation from internal combustion engines (ICE) to fully electric vehicles (EVs) is not possible due to technical limitations in battery technology, charging network, and consumer demand; different hybrid electric vehicles (HEVs) are seen as transition phase solutions. HEVs use both electric and internal combustion engines, and the fraction of different engines used depends on the type of HEV. Plug-in Hybrid Electric Vehicles (PHEVs) are seen as the most advanced HEV-type vehicles, as they can drive dozens of kilometers with only the electric

engine and thus producing less GHG and particulate emissions than ICE vehicles or other types of HEVs.

An important technology in the passenger vehicle sector to meet low exhaust-originated CO₂ emission factors has been the implementation of different types of HEV technologies. Hybrid vehicles can be divided into technologies that can be charged from the power grid and that cannot be. PHEVs are charged from the power grid and their battery capacity is about one tenth of an EV, which means that some 50 km (about 30 mi) can be driven, in theory, without starting the ICE. However, the PHEVs powertrain settings can be controlled so that occasionally electric and combustion engines are running in parallel. In the end, the driving style, chosen settings and ambient environmental parameters affect the running time of the ICE. Overall, the percentage of PHEVs among all

* Corresponding author.

E-mail address: panu.karjalainen@tuni.fi (P. Karjalainen).

¹ Present address: Emission Control and Sustainable Fuels Team, VTT Technical Research Centre of Finland, Tietotie 4 C, 02150 Espoo, Finland

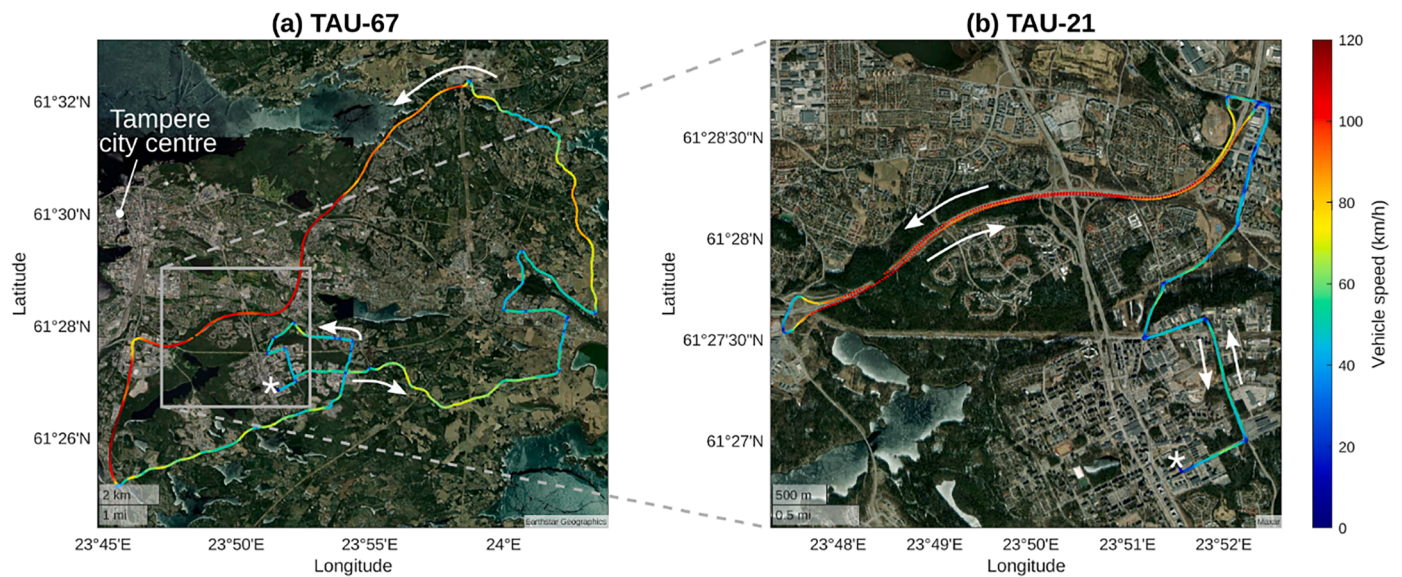


Fig. 1. Aerial maps of the driven PEMS routes, (a) TAU-67 and (b) TAU-21, with typical vehicle speeds. The asterisk denotes the location of the start and end points of the routes. Map data hosted by Esri; Sources: Earthstar Geographics, Maxar.

vehicles is still relatively low, being 0.6% in the UK (Department for Transport and Driver and Vehicle Licensing Agency, 2022) and 1.3% in Germany (Kraftfahrt-Bundesamt, 2022) in year 2021. In many countries the percentage is however increasing at a fast pace. In the UK and Germany, the share of newly registered PHEVs increased from 2020 to 2021 by 92.3% and 62.3%, being 4.1% and 12.4% in year 2021 (Department for Transport and Driver and Vehicle Licensing Agency, 2022; Kraftfahrt-Bundesamt, 2022), respectively. In Finland, the PHEV share of new registrations of vehicles was over 20% in 2021 (Traficom, 2022). This increasing market share makes the real-world emissions from these novel HEV technologies especially interesting and highly relevant to future scenarios.

The real-world fuel consumption of PHEV vehicles has been studied e.g., by Plötz et al., 2021. They report real-world CO₂ emissions for PHEVs of, on average, 50–300 $\frac{gCO_2}{km}$ (including vehicles used privately and in companies). Similarly, the actual fuel consumption for privately used vehicles was two to four times higher than test cycle consumption, “mainly due to low charging frequency” (Plötz et al., 2021). Fuel consumption of vehicles is highly dependent on the driving mode and conditions. Feinauer et al., 2022 noted that the average consumption in motorway could be 50% higher than in urban roads and within their 55 km (about 34 mi) test route the total consumption could be 15% higher in cold autumn weather than in summer. Naturally, higher fuel consumption affects emissions. The fuel consumption and the emissions were also affected by the driving mode of the PHEV. The mode with more constant ICE operation consumed more fuel but released less particle number (PN, over 23 nm non-volatile in their study) and NO_x emissions, which was speculated to be due to increased emissions in ICE ignition, which can occur multiple times during the drive. This was also seen by Ehrenberger et al., 2020 who compared emissions in different driving modes and with varying state-of-charge of the battery. They concluded that emission benefits of PHEVs are difficult to estimate, and more data are needed for defining the emissions reduction potential of this vehicle type. They also found out that cold starts of ICE during acceleration (after longer electrical driving phases) can produce a significant fraction of total emissions in terms of both NO_x and PN (over 23 nm, non-volatile).

On-road real drive emissions (RDE) testing is crucial for accurately assessing vehicle pollution levels. Laboratory testing of emissions provides valuable information but may not accurately reflect real-world driving conditions. Constant or mildly variable driving test cycles do

not provide valuable information on elements of true drive, such as acceleration, braking, and full stops, which affect total emissions. For example, Tansini et al., 2022 noted that the CO₂ emissions in real drive of PHEV may vary greatly from the standardized cycle. In addition, Prati et al., 2021 noted that CO, CO₂ and NO_x emissions are strongly affected by driving mode of the PHEV. However, number of studies on particulate emissions of PHEVs is low and they mainly concentrate on the total mass of particles or solely on the number of solid particles larger than 23 nm in size (e.g., Ehrenberger et al., 2020; Wang et al., 2021). By using RDE testing, researchers can gain a better understanding of how vehicles perform under real-world driving conditions and work towards reducing harmful emissions. This information can be used to identify areas where emissions can be reduced, develop more accurate emission models, and better control strategies.

PHEVs operate predominantly as electric vehicles with intermittent assistance from the ICE, which means that formation of the total tailpipe emission of a PHEV is not straightforward. As the vehicle tries to optimize its fuel usage, the ICE repeatedly starts and stops during the drive. This, in turn, leads potentially to multiple cold starts, which can cause drastic peaks in the emissions (Premnath and Khalek, 2019). The reason for this is that the engine start-up requires substantial fuel enrichment in gasoline vehicles, which can lead to a rise in particle formation. In addition, catalyst underperformance and ICE starting under less-than-ideal conditions may have a significant impact on tailpipe emissions. A recent article (Zhai et al., 2023) presented that a PHEV generated 43.4% less CO₂, 77.7% less NO_x than a conventional gasoline vehicle; however, it generated 183.6% more CO and 15.8% more PN (over 23 nm, non-volatile). Additionally, preheating the engine and catalyst was observed to decrease trip emissions. Another article presented high emission rates of PN and particle mass (PM) which have been observed on freeway driving speeds with bi-modal non-volatile particle size distributions, modes peaking at 9 nm and 30 nm (Yang et al., 2021). Furthermore, (Li et al., 2021) noted that re-ignition events can cause cold-start-like high emissions when the engine is re-ignited after being cooled while turned off, especially as the engine cools off faster under cold weather conditions.

In this study, we will show the emission factors (EFs) from a PHEV in different driving conditions and situations and compare them to emissions from conventional gasoline vehicles using only ICE powertrain. The study focuses on the trend in emissions profiles of signature gasoline engine technologies of the past decade; changing first from PFI to GDI

Table 1
Details of test vehicles: model, year, mileage, emission classification, engine and aftertreatment systems employed. Numbers of rounds measured in different routes and with cold and hot start, the durations of measurements, and mean speeds for each vehicle are also listed.

Vehicle	Model year	Mileage (km)	Emission class	Engine	Aftertreatment	Number of measurements on TAU-67 (cold/hot)	Duration of measurements on TAU-67 (min; max, mm. ss)	Mean speed on TAU-67 (min; max, km/h)	Number of measurements on TAU-21 (cold/hot)	Duration of measurements on TAU-21 (min; max, mm. ss)	Mean speed on TAU-21 (min; max, km/h)
VW Passat	2017	76 000	Euro 6	Gasoline Hybrid PHEV (1.4 GDI)	TWC	1/1	65.32; 68.29	59.06; 61.73	1/5	22.55; 26.08	47.65; 54.36
Kia	2014	87 000	Euro 5	1.6 GDI	TWC	1/1	79.16; 80.22	50.34; 50.92	1/1	25.47; 27.35	45.00; 47.02
Ford Focus	2010	144 000	Euro 5	1.6 PFI	TWC	1/1	70.12; 70.34	57.36; 57.56	1/1	26.03; 26.10	47.74; 48.04

and then to hybrid powertrains. We will present the temporal behavior of multiple properties of detailed particle emissions, such as PN (down to 2.5 nm, both volatile and non-volatile), PM, particle size distribution and BC, which were characterized for PHEV and ICE vehicles under different driving conditions with a portable emissions measurement system (PEMS). The drive includes different operating settings of the PHEV which affect the usage of ICE at various stages of the test routes.

Experimental

Driving route and test vehicles

Two driving routes were used. Driving routes vary greatly in the means of driving conditions and thus of emissions. Longer route (TAU-67) is a 67 km route (Fig. 1(a)), consisting of typical urban driving (0–60 km/h), driving with moderate speeds (60–80 km/h) and a total of 25 km motorway driving (~100 km/h). Shorter route (TAU-21) is total of 21 km (Fig. 1(b)), consisting of typical urban driving and 10 km of motorway driving.

Table 1 introduces the vehicles used. Vehicles were measured with cold and hot start. Before a cold start test, the vehicle was soaked overnight and the time from the last drive or measurement was at least 16 hours. For practical reasons, hot start rounds were performed after a cold start round.

The weather during the measurements was typical Finnish summer weather, temperature ranging between 10 and 20 °C and hourly rainfall between 0 and 2.3 mm. Measurements were conducted between 9 am and 3 pm, when the other traffic count was relatively low.

Both the weather and traffic conditions were relatively similar during the measurement days. The Figure S1 shows that the temperature and rain profile during measurement days was relatively stable, i.e. temperature and rain conditions during the first round (i.e. a cold start measurement) of each day was not very much different from the other measurement rounds. Also, the measurement duration was relatively stable between different measurement rounds, as can be seen from Table 1, that is listing the minimum and maximum durations for each measurement route – vehicle combination. The largest relative difference was between the fastest and the slowest round was 14% in VW Passat short route measurements (shortest round of six rounds was 22 min 55 seconds, longest 26 minutes 8 seconds). For all the other vehicle – measurement route combinations the relative differences were smaller.

Measurement setup

The PEMS system (TAU-PEMS) was applied on-board the test vehicles in the experimental runs. The PEMS consists of a main unit inside the vehicle and a tailpipe sampling unit installed outside the vehicle (Järvinen et al., 2015; Martikainen et al., 2020). The system was powered by its own lithium batteries during the studies; usually with the used consumption the batteries can operate continuously about 5 h. In the PEMS measurements, exhaust gas was sampled from the tailpipe and immediately diluted with cool dilution at ambient temperature in a porous tube diluter (PTD, dilution ratio (DR) set to approximately 12). After primary dilution, the sample was taken into a residence time tube (1.5 s) followed by an ejector diluter (DR 6). The required dilution air was passed through activated carbon and HEPA filters and was free of particle phase impurities. This special miniature type-sampling system involving a PTD is assumed to mimic delayed primary particle formation occurring in a real exhaust plume behind a vehicle upon cooling of the exhaust, as it is generally thought to be mimicked with other PTD-involving sampling systems of traditional sizes (Ntziachristos et al., 2004). CO₂ measured by sensors (GMM111 and GM112, Vaisala Oyj, Finland) was used as a tracer for fuel consumption and to determine the DR of the sampling system. The vehicle specific parameters were logged via the on-board diagnostic OBD-II protocol using Easylogger software.

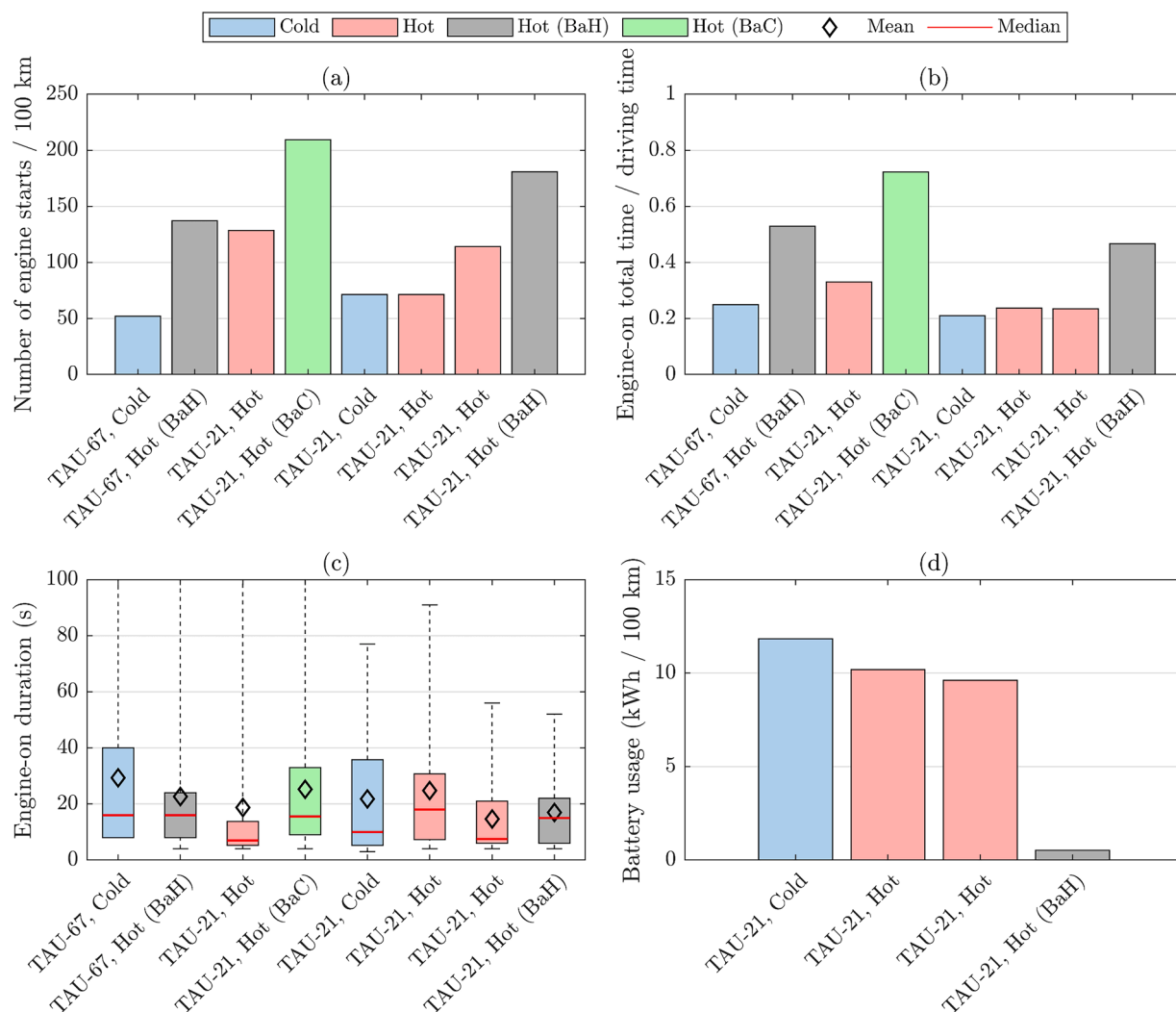


Fig. 2. Statistics of the PEMS measurement drives for the PHEV vehicle with three different driving modes: normal hybrid, battery hold (BaH) and battery charge (BaC), and with initially cold or hot engine. Most of the drives are from the shorter, TAU-21 route. Subplots (a) - (c) also include two drives from the longer, TAU-67 route. Engine-on durations represent the durations of ICE running at once; the box represents the quartiles (1st quartile, median, and 3rd quartile). The whiskers show the minimum and maximum engine-on duration. Four leftmost whiskers in subplot (c), that are outside the scale of the y axis, reach approximately 170, 135, 145, and 135 seconds, respectively.

This allowed for the selection of 8 parameters from the engine OBD channel to be logged during the drives.

The diluted exhaust sample was drawn to the measuring instruments, which were an Ultrafine Condensation Particle Counter (CPC 3756, TSI Inc., USA; 1.5 l/min flow rate, 1 s time resolution) for PN, another Ultrafine CPC (CPC 3776, TSI Inc., USA; 1.5 l/min flow rate, 1 s time resolution) downstream a catalytic stripper (catalyst as in AVL PN PEMS, losses presented in (Samaras et al., 2022)) operated at 350°C for non-volatile PN, a dual-spot aethalometer AE33 (Aerosol Co., Slovenia; 5.0 l/min) (Drinovec et al., 2015) for BC, and an Engine Exhaust Particle Sizer (EEPS 3090, TSI Inc., USA; 10 l/min, 1 s time resolution, SOOT inversion matrix) (Xue et al., 2016) for particle size distributions. The EEPS particle size distributions were used to calculate PM concentrations by taking only particles smaller than 300 nm into account. This upper limit was used because noise in the particle bins above this limit would dominate PM. Upstream the CPC, an additional passive dilution bridge was needed (DR 97). The CO₂ emissions were measured by LI-840A (LI-COR Inc., USA) instrument.

Emission factor calculation

The emission factors (per km) were calculated by summing second by

second (if such data was available) multiplication of the concentration and the exhaust flow rate over the whole drive. If the second-level data were not available (as was the case in some drives), the sum of the concentration over the drive was multiplied with the mean exhaust flow rate of the drive. The obtained values were then corrected with the dilution ratio of the sampling setup and with the lengths of the drives in kilometers. Because the latter method was observed to result in underestimated emission factors, the emission factors calculated with that were corrected with vehicle-specific scaling factors obtained separately for every test vehicle. The estimation of engine parameters, such as the exhaust flow rate, was based on the OBD data. The measurement device data were recorded with a one-second time resolution. The PM mass (size range 5.6–300 nm) was calculated from the EEPS.

Results and discussion

The results shown here inspect thoroughly when the emissions from a PHEV are released and what are the main causes for them. We will also compare the PHEV emissions to similar drives with two vehicles with conventional ICE. The emissions of a PHEV depend greatly on the driving mode of the vehicle, battery level, and driving conditions, which all affect the number of ignitions and required run time of the ICE. These

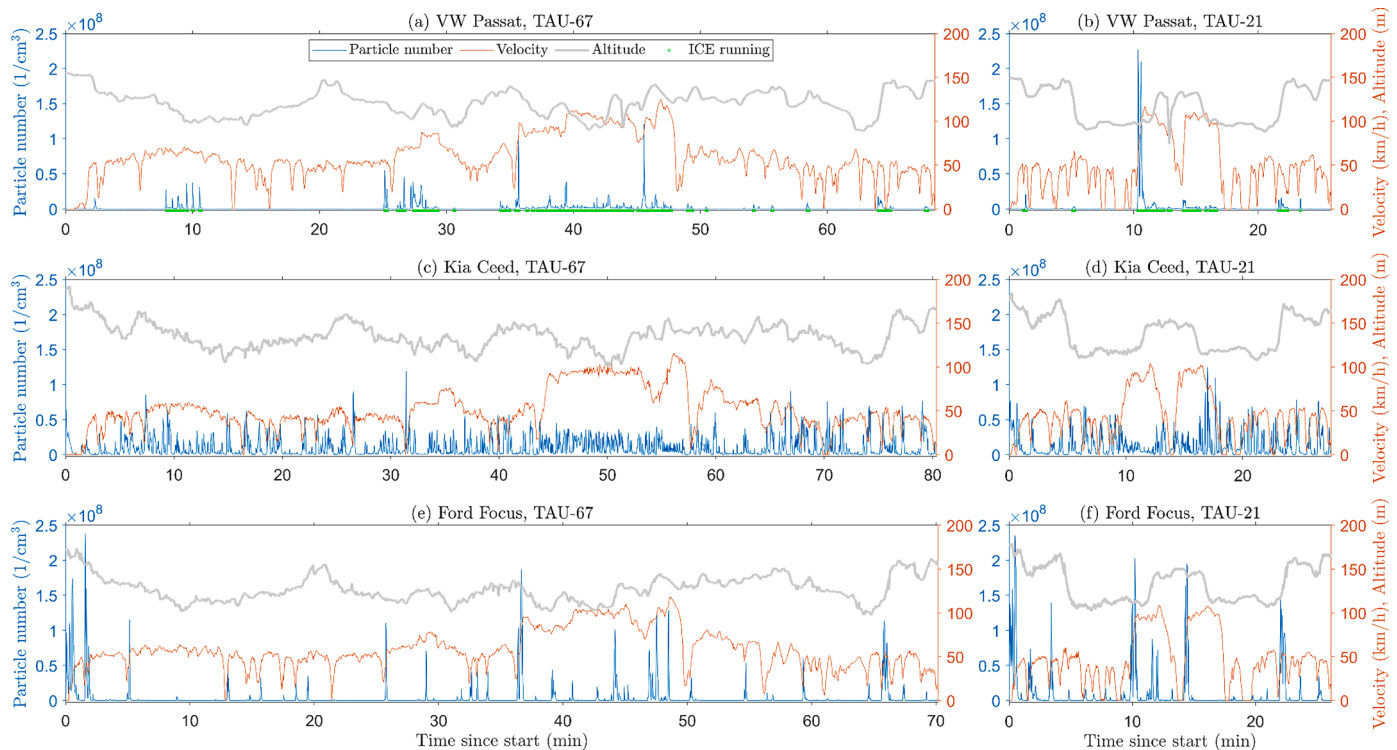


Fig. 3. Example time series of particle number, velocity, and altitude for longer TAU-67 route for VW Passat PHEV (a), Kia Ceed (c) and Ford Focus (e), and for shorter TAU-21 route (b, d and f respectively). For VW Passat PHEV the running times of Internal Combustion Engine (ICE) have been marked with green dots. All drives (a-f) were driven with an initially cold engine. VW Passat was driven with the “hybrid” mode selected by the driver.

aspects are examined in the following sections.

Under normal driving conditions in the hybrid mode, the hybrid vehicle starts and stops the ICE operation depending on the acceleration pedal use of the driver. If the vehicle accelerates rapidly the PHEV can use the additional power from the ICE together with the electrical engine. This may also affect reversely, meaning that when driving with ICE, the electrical engine can take part of the load needed for acceleration and thus reduce fuel consumption and emissions. In addition, the ICE ignition frequency can depend on the remaining battery level. The used VW Passat had three modes: a hybrid mode, using mostly the electric engine, battery-hold (BaH) mode in which the vehicle was trying to maintain the battery level while driving, and battery-charge (BaC) mode in which the vehicle was mainly using the ICE and charging the vehicle battery.

Fig. 2 shows statistics, i.e., number of ICE starts, ICE engine on time fraction, distribution of engine on duration, and battery usage for different drives. The number of ICE starts and the fraction of engine-on total time is, on average, higher for BaH and BaC modes than for the normal hybrid mode. Engine-on duration has quite similar distribution independently on the used battery mode having the mean of 15–30 seconds engine-on time after ignition. The battery usage, that was measured only for the last four drives, shows that for normal hybrid mode battery usage has been significant, whereas for BaH mode the battery usage has been almost negligible, as is also expected.

Fig. 3 illustrates the variation in driving speed and altitude and their effect on particle emissions for the three vehicles studied. The figure clearly shows the effect of higher load on engine during accelerations and uphill driving, and specifically the effect of accelerations and uphill driving on PHEV’s ICE operation. The PHEV, operated in hybrid mode in Fig. 3 (a) and (b), showed the ICE was started mainly when the vehicle was accelerating or driving uphill. The ICE was running during the freeway driving and the steep Lukonmäki uphill just before the end of the routes (~65 min at TAU-67 and ~22 min at TAU-21). There were few ignitions that were not related to notable accelerations or uphill

driving in both drives (a and b), which may be caused by the ICE starting when the battery charge needed maintaining or the vehicle tries to balance between the fuel consumption and battery usage.

Kia Ceed, equipped with a GDI engine, emitted notable PN concentrations continuously and released the highest total PN emissions during the drive in both routes (Fig. 3 c and d) whereas the Ford Focus, with PFI engine, showed noticeable PN peaks only during accelerations and when driving uphill.

The driving mode of PHEV affects greatly the ICE starting and stopping and thus its emissions. During hybrid mode ICE was mainly used for motorway driving and large uphill towards the end of the drive. During BaH mode, ICE was also used during almost every acceleration and some stable driving periods with lower speed (~50 km/h). During BaC mode, ICE was used almost during the entire drive: ICE was off only when the speed was decreasing rapidly, i.e., when the battery was recharged by braking. The number of starts was higher during BaH and BaC mode drives than during the hybrid mode drive.

Fig. 4 shows that the ICE ignition causes an immense peak in the particle number. The peaks are drastically higher than emissions from constant drive and thus ICE ignitions cause a large fraction of total emissions of the drive. The highest peaks in emissions could be seen when the vehicle was accelerating onto the motorway, except in the BaC drive where the highest emission of primary particles was released when the vehicle was driving uphill on the motorway. Overall, the figure seems to indicate that the number of particles emitted are rather dependent on the ICE engine-on time which naturally follows the decreasing order of BaC, BaH, and hybrid.

The plots also contain information of particle number properties, including the total (fresh) and non-volatile (primary) fractions (measured downstream a catalytic stripper). We observe that both particle number fractions are in a very good correlation indicating the lack of semi-volatile new particles formed during the dilution process executed at the ambient temperature.

Since the particle number information does not cover all the

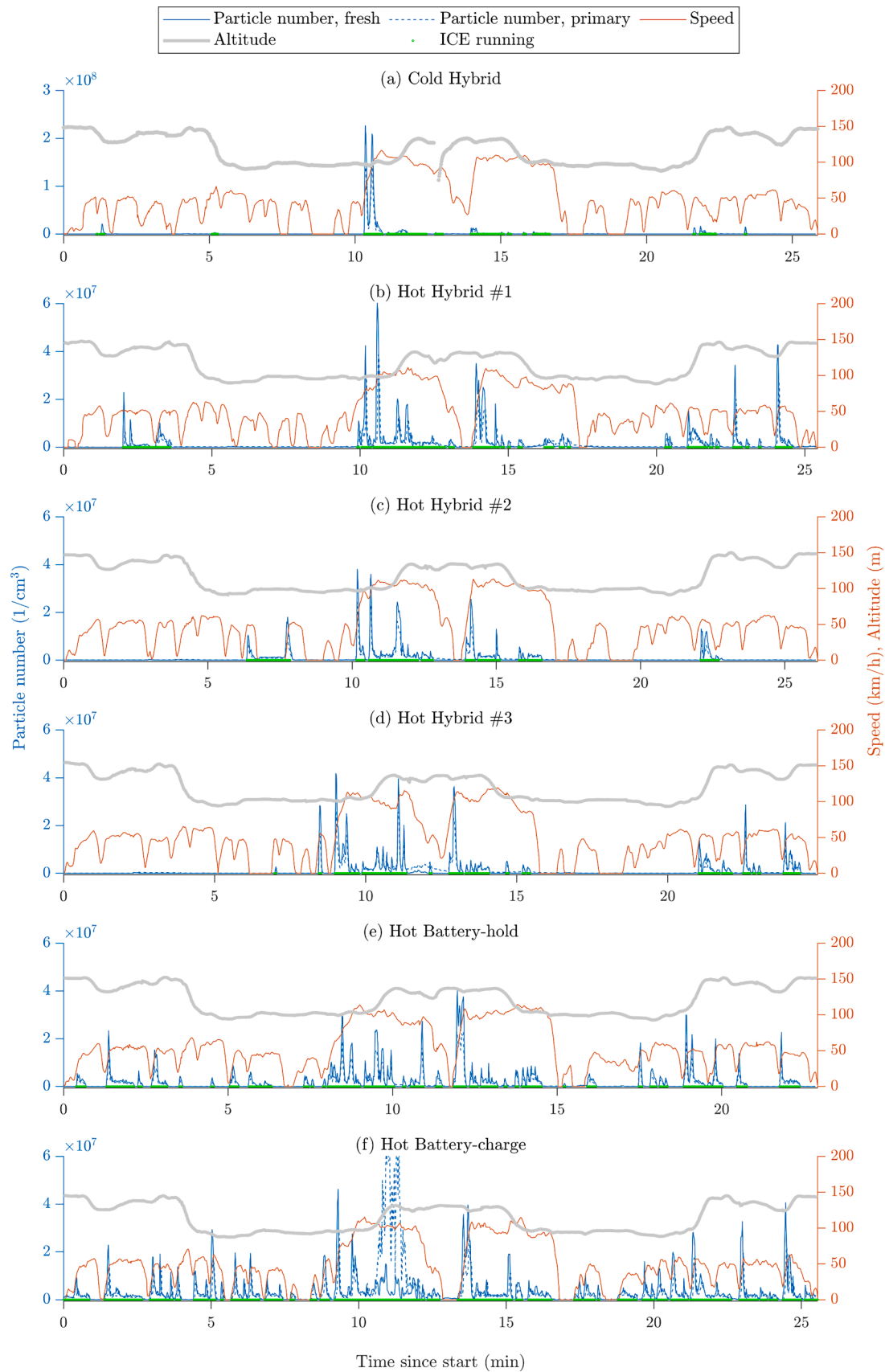


Fig. 4. Time series of particle number, velocity, altitude, and the running state of Internal Combustion Engine for all shorter route (TAU-21) drives of VW Passat PHEV. Different EV options ("hybrid" (a-d), "battery-hold" (e), and "battery-charge" (f)) and initial engine temperatures (cold, hot) were used. The running times of Internal Combustion Engine (ICE) have been marked with green dots. Drive (a) was driven with an initially cold engine, and the rest (b-f) with a hot engine. Note that the left y-axis scale is 5 times wider for subfigure (a) than for the rest of the subfigures.

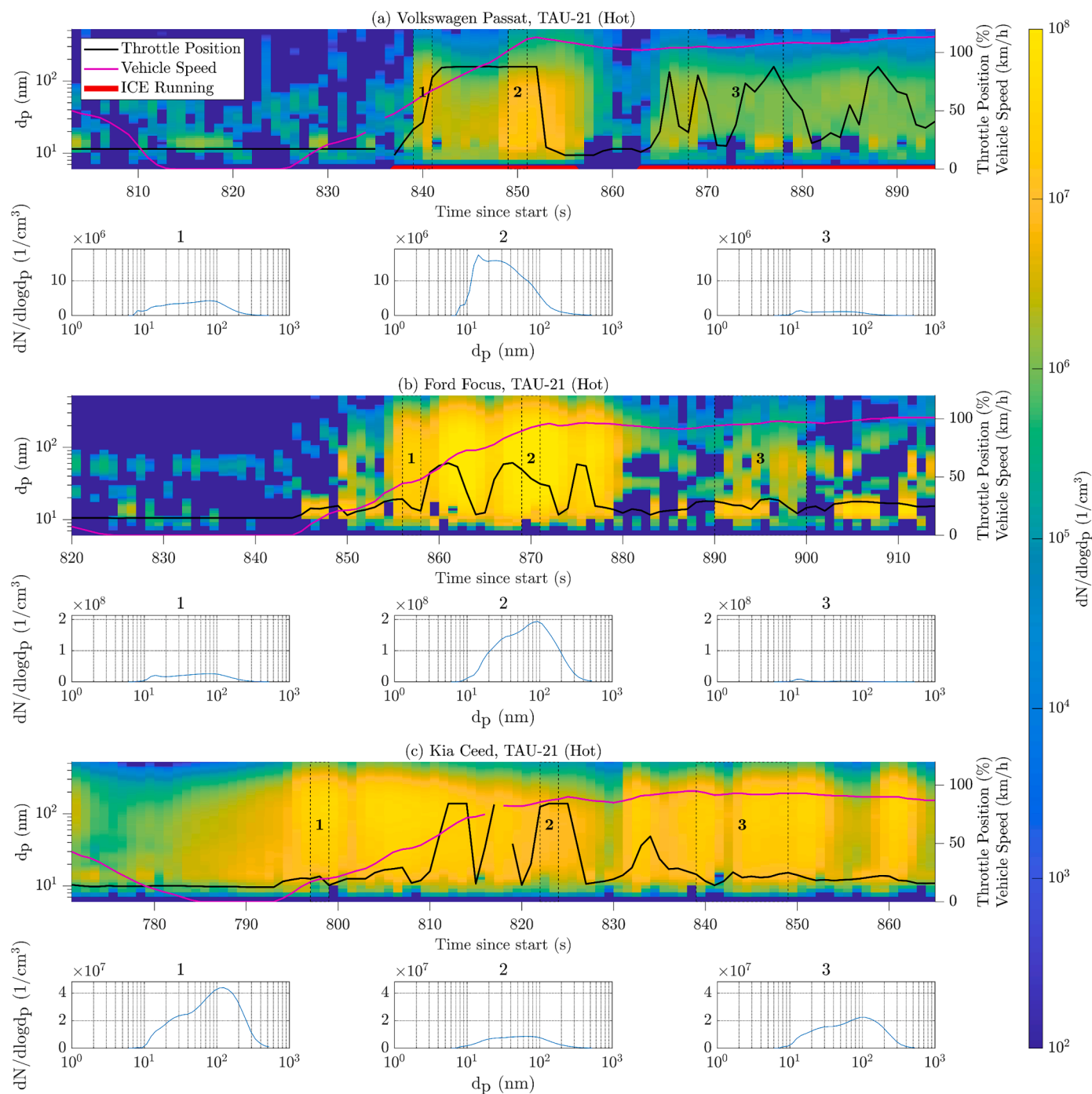


Fig. 5. Time series of particle number-size distribution during the acceleration to motorway for VW Passat PHEV (subplot a), Ford Focus (b), and Kia Ceed (c). For VW Passat PHEV the running times of Internal Combustion Engine (ICE) have been marked with red line. Snapshot size distributions (below the main particle number-size distribution plot) are represented for short periods for each vehicle from the beginning of the acceleration (number 1), when the vehicle reached motorway speed (2), and during the stable speed on the motorway (3).

properties of the particle size distribution, we used the EEPS to measure the temporal profile of particle size distributions during the drives. Fig. 5 shows the number size distributions of particles measured by EEPS during the acceleration to the motorway in the TAU-21 route approximately 13–14 minutes from the start of the measurement. Size distributions show clear differences between the particle number emissions of GDI and PFI vehicles that were also shown in Fig. 3: GDI vehicles (Kia Ceed, VW Passat) have continuous emission of particles (for VW Passat, during ICE-on time), whereas the PFI vehicle (Ford Focus) is emitting a notable number of particles only during the accelerations. When the

stable speed was reached in the motorway (e.g., period 3 in Fig. 5b) Ford Focus mainly emitted small, approximately 10–20 nm particles. During acceleration, Ford Focus also emitted larger particles. For Kia Ceed, the particle size distribution does not have such a dependence, and for VW Passat the dependence is not very clear. Some milder accelerations for VW Passat (e.g., 875–880 seconds from the start) show higher emissions for smaller particles, but the shape of the size distribution at period 3 does not differ significantly from the size distributions at points 1 and 2.

When looking at a series of tests, EFs from total particle number, nonvolatile particle number, particle mass and black carbon vary greatly

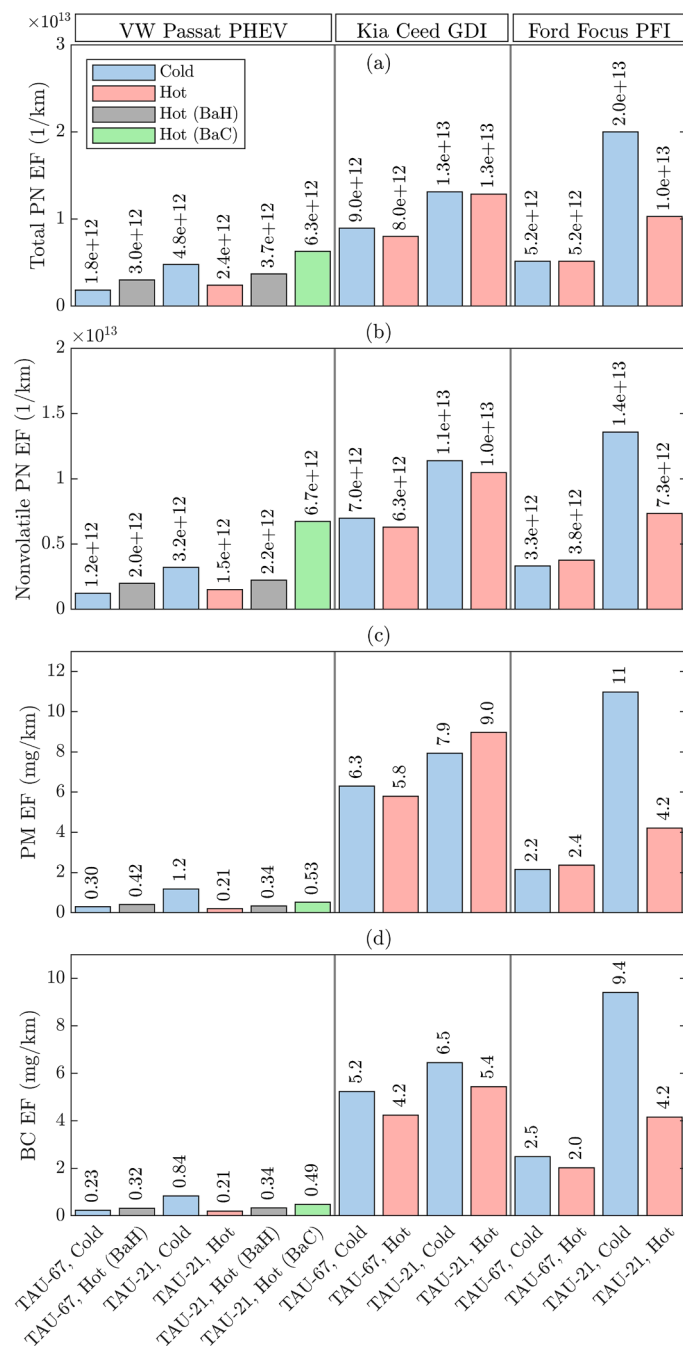


Fig. 6. Emission factors (EFs) for total PN over 2.5 nm (1st panel), nonvolatile PN over 2.5 nm (2nd panel), PM under 300 nm (3rd panel) and BC (4th panel), for VW Passat, Kia Ceed, and Ford Focus during different driving routines, respectively

between vehicles, routes, test drives, and different driving modes of the PHEV. The results presented in Fig. 6 demonstrate the variation in EFs for three vehicles under various driving conditions. The EFs for the VW Passat PHEV were consistently the lowest among the three vehicles, with the Ford Focus (PFI) emitting more than the PHEV, and the Kia Ceed (GDI) emitting the most. The similarity in profiles between the total and non-volatile components of particle number emissions indicates that there is a lack of semi-volatile dilution-formed particles for all three vehicles. Interestingly, the PHEV vehicle's emissions were comparable to those of the other vehicles when PN properties were considered, as well as in the scale of (Feinauer et al., 2022) that reported emissions factor of $9e+11$ 1/km for nonvolatile particles larger than 10 nm.

However, PM and BC emissions were much lower than those of the conventional gasoline vehicles due to the smaller particle size, as shown in Fig. 5.

The strong relation between PM and BC emissions indicates the dominance of BC in the particle composition of all three vehicles. While PM is not entirely composed of BC, it does provide a good indication of the total PM content. The GDI had a smaller fraction of BC than the other two vehicles. The cold start effect on all emissions (PN, PM, BC) was found to be significant for the PHEV and the PFI at the TAU-21 route, but not for the GDI. The effect of cold start on emissions was negligible for all vehicles at the TAU-67 route.

Finally, the VW Passat showed the highest EFs for BaC, cold start hybrid, and BaH drives, respectively. The high EFs of the cold hybrid drive in the TAU-21 route was mainly due to the ICE ignition during acceleration to the motorway. In the TAU-67 route, however, cold start emissions in hybrid drive did not show a significant difference when compared to hot engine drive in BaH mode. These results provide insight into the variation in emission factors for different vehicles and driving conditions, which can be valuable in developing emission control strategies for reducing air pollution.

Conclusions

Our study focused on examining the particle emissions of a plug-in hybrid vehicle (VW Passat) compared to two conventional gasoline vehicles, namely the PFI (Ford Focus) and GDI (Kia Ceed) vehicles. We compared the distance-based emission factors for each vehicle in various driving modes, including battery-hold and battery-charge driving modes for the PHEV.

Our results showed that the plug-in hybrid engine produced smaller particles in size than the PFI and GDI engines, resulting in significantly lower PM and BC emission factors based on distance. Furthermore, the distance-based emission factors for the plug-in hybrid engine were consistently lower than those of the PFI and GDI engines in all driving modes, including the consuming battery-charge mode.

Regarding the vehicle cold start effect, we found that it was present in the case of the short route (TAU-21) but not as significant in the longer route (TAU-67). This is natural due to relatively longer time when the engine is cold after the start of the drive in the short route. For the long route, we did not observe any case where the cold start of the engine was in a major role in total emission factor.

In conclusion, our study demonstrated that plug-in hybrid vehicles can produce lower particle number and mass emissions and black carbon mass emissions compared to traditional gasoline-powered vehicles. Furthermore, the vehicle cold start and systematic restart effects can have a significant impact on particle emissions, especially in shorter trips. Therefore, we recommend that drivers of plug-in hybrid vehicles avoid heavy acceleration to minimize ICE ignition events and hence their environmental impact. On the other hand, PHEV manufacturers could consider more frequent programming of the powertrain to prioritize sustained operation of the internal combustion engine (ICE), with the electric motor being restarted as needed. This stands in contrast to the current approach, where the ICE is frequently reignited, and the electric motor is kept in more constant operation, as observed in practices adopted by some manufacturers.

Regarding aforementioned conclusions, we acknowledge the limitation of the study having a small sample size, and the vehicles compared are not from the same make. However, with these measurements, we were able to inspect the emissions more deeply and have an overview of the trends in emissions profiles of signature gasoline engine technologies.

CRedit authorship contribution statement

P. Karjalainen: Conceptualization, Data curation, Formal analysis, Investigation, Methodology, Writing – original draft, Project

administration, Resources, Visualization, Supervision, Funding acquisition. **V. Leinonen:** Conceptualization, Writing – review & editing. **M. Olin:** Conceptualization, Data curation, Formal analysis, Investigation, Methodology, Writing – original draft, Project administration, Visualization. **K. Vesisenaho:** Data curation, Writing – original draft, Visualization. **P. Marjanen:** Investigation, Writing – review & editing. **A. Järvinen:** Methodology, Investigation, Writing – review & editing. **P. Simonen:** Investigation, Writing – review & editing. **L. Markkula:** Investigation, Writing – review & editing. **H. Kuuluvainen:** Investigation, Writing – review & editing. **J. Keskinen:** Investigation, Writing – review & editing, Funding acquisition. **S. Mikkonen:** Conceptualization, Writing – original draft, Project administration, Resources, Supervision, Funding acquisition.

Declaration of Competing Interest

The authors declare that they have no known competing financial interests or personal relationships that could have appeared to influence the work reported in this paper.

Data availability

Data will be made available on request.

Funding

This research is part of the Academy of Finland project “EFFi” (grant no. 322120), and supported by the “AHMA” project funded by the Jane and Aatos Erkko’s Foundation. P.K. acknowledges funding from Tampere Institute for Advanced Study (Tampere IAS). S.M. is supported by the Academy of Finland competitive funding to strengthen university research profiles (PROFI) for the University of Eastern Finland (grant nos. 325022 and 352968). This research has received support from the Academy of Finland Flagship Programme “ACCC” (grant nos. 337550 and 337551).

Supplementary materials

Supplementary material associated with this article can be found, in the online version, at [doi:10.1016/j.envadv.2023.100454](https://doi.org/10.1016/j.envadv.2023.100454).

References

- Department for Transport and Driver and Vehicle Licensing Agency, 2022. Cars (VEH02) - GOV.UK [WWW Document]. <https://www.gov.uk/government/statistical-data-sets/veh02-licensed-cars> (accessed 3.30.22).
- Drinovec, L., Močnik, G., Zotter, P., Prévôt, A.S.H., Ruckstuhl, C., Coz, E., Rupakheti, M., Sciare, J., Müller, T., Wiedensohler, A., Hansen, A.D.A., 2015. The “dual-spot” Aethalometer: an improved measurement of aerosol black carbon with real-time loading compensation. *Atmos. Meas. Tech.* 8, 1965–1979. <https://doi.org/10.5194/amt-8-1965-2015>.
- Ehrenberger, S.I., Konrad, M., Philipps, F., 2020. Pollutant emissions analysis of three plug-in hybrid electric vehicles using different modes of operation and driving conditions. *Atmos. Environ.* 234, 117612 <https://doi.org/10.1016/j.atmosenv.2020.117612>.
- Feinauer, M., Ehrenberger, S., Eppe, F., Schripp, T., Grein, T., 2022. Investigating Particulate and Nitrogen Oxides Emissions of a Plug-In Hybrid Electric Vehicle for a Real-World Driving Scenario. *Appl. Sci. (Switzerland)* 12. <https://doi.org/10.3390/app12031404>.
- Järvinen, A., Rostedt, A., Wihersaari, H., Olin, M., Yli-Ojanperä, J., Rönkkö, T., Keskinen, J., 2015. Portable Emission Measurement System (PEMS) for Exhaust Aerosols. In: *ETH Nanoparticles Conference (NPC)*.
- Kraftfahrt-Bundesamt, 2022. Kraftfahrt-Bundesamt - Pressemitteilungen - Der Fahrzeugbestand am 1. Januar 2022 [WWW Document]. https://www.kba.de/DE/Presse/Pressemitteilungen/Fahrzeugbestand/2022/pm10_fz_bestand_pm_komplett.html?snn=3662144 (accessed 3.30.22).
- Li, C., Swanson, J., Pham, L., Hu, Shaohua, Hu, Shishan, Mikailian, G., Jung, H.S., 2021. Real-world particle and NOx emissions from hybrid electric vehicles under cold weather conditions. *Environ. Pollut.* 286, 117320 <https://doi.org/10.1016/j.envpol.2021.117320>.
- Martikainen, S., Karjalainen, P., Rönkkö, T., Järvinen, A., Kalliokoski, J., Keskinen, J., Ntziachristos, L., Teinilä, K., Saarikoski, S., Aurela, M., Timonen, H., Saveljeff, H., Lauren, M., 2020. Characterization of Physical and Chemical Properties of Particulate Emissions of a Modern Diesel-Powered Tractor under Real Driving Conditions. In: *SAE Technical Papers*. <https://doi.org/10.4271/2020-01-2204>.
- Ntziachristos, L., Giechaskiel, B., Pistikopoulos, P., Samaras, Z., Mathis, U., Mohr, M., Ristimäki, J., Keskinen, J., Mikkonen, P., Casati, R., Scheer, V., Vogt, R., 2004. Performance Evaluation of a Novel Sampling and Measurement System for Exhaust Particle Characterization. In: *SAE Technical Papers*. <https://doi.org/10.4271/2004-01-1439>.
- Plötz, P., Moll, C., Bieker, G., Mock, P., 2021. From lab-to-road: real-world fuel consumption and CO2 emissions of plug-in hybrid electric vehicles. *Environ. Res. Lett.* 16, 054078 <https://doi.org/10.1088/1748-9326/ABEF8C>.
- Prati, M.V., Costagliola, M.A., Giuzio, R., Corsetti, C., Beatrice, C., 2021. Emissions and energy consumption of a plug-in hybrid passenger car in Real Driving Emission (RDE) test. *Transp. Eng.* 4, 100069 <https://doi.org/10.1016/j.treng.2021.100069>.
- Premnath, V., Khalek, I., 2019. Particle Emissions from Gasoline Direct Injection Engines during Engine Start-Up (Cranking), in: *SAE Technical Papers*. SAE International. <https://doi.org/10.4271/2019-01-1182>.
- Samaras, Z., Rieker, M., Papaioannou, E., van Dorp, W.F., Kousoulidou, M., Ntziachristos, L., Andersson, J., Bergmann, A., Hausberger, S., Keskinen, J., Karjalainen, P., Martikainen, S., Mamakos, A., Haisch, C., Kontses, A., Toumasatos, Z., Landl, L., Bainschab, M., Lähde, T., Piacenza, O., Kreutziger, P., Bhave, A.N., Lee, K.F., Akroyd, J., Kraft, M., Kazemimanesh, M., Boies, A.M., Focsa, C., Duca, D., Carpentier, Y., Pirim, C., Noble, J.A., Lancry, O., Legendre, S., Tritscher, T., Spielvogel, J., Horn, H.G., Pérez, A., Paz, S., Zarvalis, D., Melas, A., Baltzopoulou, P., Vlachos, N.D., Chasapidis, L., Deloglou, D., Daskalos, E., Tsakis, A., Konstandopoulos, A.G., Zinola, S., Di Iorio, S., Catapano, F., Vaglieco, B.M., Burtcher, H., Nicol, G., Zamora, D., Maggiore, M., 2022. Perspectives for regulating 10 nm particle number emissions based on novel measurement methodologies. *J. Aerosol Sci.* 162, 105957 <https://doi.org/10.1016/j.jaerosci.2022.105957>.
- Tansini, A., Pavlovic, J., Fontaras, G., 2022. Quantifying the real-world CO2 emissions and energy consumption of modern plug-in hybrid vehicles. *J. Clean. Prod.* 362, 132191 <https://doi.org/10.1016/j.jclepro.2022.132191>.
- Traficom, 2022. First registrations of passenger cars by Area, Model, Driving power and Month. PxWeb [WWW Document]. URL https://trafi2.stat.fi/PXWeb/pxweb/en/TraFi/TraFi_Ensirekisteroinnit/050_ensirek_tau_105.px (accessed 3.30.22).
- Wang, Y., Wang, J., Hao, C., Wang, X., Li, Q., Zhai, J., Ge, Y., Hao, L., Tan, J., 2021. Characteristics of instantaneous particle number (PN) emissions from hybrid electric vehicles under the real-world driving conditions. *Fuel* 286. <https://doi.org/10.1016/j.fuel.2020.119466>.
- Xue, J., Li, Y., Quiros, D., Wang, X., Durbin, T.D., Johnson, K.C., Karavalakis, G., Hu, S., Huai, T., Ayala, A., Jung, H.S., 2016. Using a new inversion matrix for a fast-sizing spectrometer and a photo-acoustic instrument to determine suspended particulate mass over a transient cycle for light-duty vehicles. *Aerosol Sci. Technol.* 50, 1227–1238. <https://doi.org/10.1080/02786826.2016.1239247>.
- Yang, Z., Zhang, X., Xie, Z., Qi, S., Wang, J., Li, J., Li, M., 2021. Research on the characteristics of real-world vehicle particle number and mass emissions. In: *IOP Conf Ser Earth Environ Sci*, 831, 012013. <https://doi.org/10.1088/1755-1315/831/1/012013>.
- Zhai, Z., Xu, J., Zhang, M., Wang, A., Hatzopoulou, M., 2023. Quantifying start emissions and impact of reducing cold and warm starts for gasoline and hybrid vehicles. *Atmos. Pollut. Res.* 14, 101646 <https://doi.org/10.1016/J.APR.2022.101646>.